Available online at www.sciencedirect.com
SCIENCE DIRECT®
International Journal of Heat and Mass Transfer 49 (2006) 3104–3110
International Journal of HEAT and MASS TRANSFER
www.elsevier.com/locate/ijhmt

A study on the kinetics of ethanol-activated carbon fiber: Theory and experiments

Ibrahim I. El-Sharkawy [a], Bidyut B. Saha [b], Shigeru Koyama [b], Kim Choon Ng [c,*]

[a] Department of Energy and Environmental Engineering, Kyushu University, Kasuga-koen 6-1, Kasuga-shi, Fukuoka 816-8580, Japan
[b] Institute for Materials Chemistry and Engineering, Kyushu University, Kasuga-koen 6-1, Kasuga-shi, Fukuoka 816-8580, Japan
[c] Department of Mechanical Engineering, National University of Singapore, 10 Kent Ridge Crescent, Singapore 119260, Singapore

Received 19 August 2005; received in revised form 3 February 2006
Available online 18 April 2006

Abstract

An experimental and theoretical study has been conducted on the adsorption kinetics of ethanol onto a pitch-based activated carbon fiber (ACF) of type (A-20). Experiments have been carried out across assorted adsorption temperatures that are useful to the operation of adsorption chillers. The kinetic curve for each isotherm is measured accurately using a thermal-gravimetric analyzer (TGA) from which the diffusion time constant and consequently, the overall mass transfer coefficient could be evaluated. A novel concentration profile, with an exponent parameter k, has been proposed in the theoretical model which accounts for the effect of meso- and micro-pore structures within the ACF. The proposed concentration profile removes the restrictions between the overall mass transfer coefficient and the diffusion time constant. Using the measured kinetics, the numerical value of k is evaluated, leading to a new form of the linear driving force (LDF) model for cylindrical adsorbent that could capture the higher ethanol uptake in ACF and this LDF model has been validated experimentally.

Keywords: Activated carbon fiber; Adsorption kinetics; Diffusion time constant; Ethanol; Linear driving force model; Overall mass transfer coefficient

1. Introduction

Activated carbon fibers (ACFs) have many intrinsic characteristics that are superior as compared with the palletized or granular activated carbon, for example, the large surface area, fast inter-particle adsorption kinetics, ease of handling and manufacture into belts or foam components. It could be used in applications such as gas separation, gas storage and catalytic reactions [1–5]. In recent years, several studies have been conducted to investigate the potential types of ACFs-refrigerant pairs in adsorption cooling or heat pump applications [6–8]. The uptake behaviour of ACF (A-20)/ethanol pair seems to be a promising for cooling applications. Besides the high affinity for ethanol, the salient features of ACF (A-20) are (i) a high surface area of about 1.95×10^6 m^2/kg, (ii) a pore volume of 10.28×10^{-4} m^3/kg and (iii) a suitable average pore diameter of approximately 21.6 Å [9,10].

For design purposes and improving the understanding of adsorption chillers, it is essential to determine accurately the kinetics of adsorbent–adsorbate (refrigerant) pair. Design codes of chiller must be equipped with the correct isotherms, isosteric heat of adsorption and the coefficients for the uptake model. With these key data furnished for the adsorbent–sorbate pair, only then the numerical modeling of the processes of chiller operation can be computed accurately with high level of degree of confidence [11]. Conventionally, the computations time of the code could be optimized using the well-known linear driving force (LDF) correlation.

In the LDF method, the key parameter employed here is the determination of the overall particle mass transfer coefficient. Both the diffusion time constant and the overall

* Corresponding author. Tel.: +65 68742214; fax: +65 67791459.
E-mail address: mpengkc@nus.edu.sg (K.C. Ng).

0017-9310/$ - see front matter © 2006 Elsevier Ltd. All rights reserved.
doi:10.1016/j.ijheatmasstransfer.2006.02.029

Nomenclature

a_0	time dependent coefficient of Eq. (7)	t	time [s]
a_2	time dependent coefficient of Eq. (7)	v	elemental volume of fiber $(2\pi rL)$[m^3]
D_s	surface diffusion coefficient [m^2/s]	v_0	volume of fiber $(2\pi RL)$ [m^3]
F_0	constant used in Eq. (1)	$\bar{w}$	average amount of adsorbate [kg/m^3 or $kg_{ethanol}/kg_{ACF}$]
k	constant used in Eq. (7)	W	equilibrium adsorption capacity [kg/m^3 or $kg_{ethanol}/kg_{ACF}$]
$K_s a_v$	overall mass transfer coefficient [s^{-1}]	D_s/R^2	diffusion time constant [s^{-1}]
L	fiber length [m]	w/W	fractional uptake [–]
r	radial distance in the fiber [m]		
R	fiber radius [m]		

mass transfer coefficient are estimated by tracking the experimental vapour-uptake behaviour using the solution of a diffusion equation where the particle mass transfer coefficient ($K_s a_v$) could be determined [12]. Should only the surface diffusion parameter D_s is used, there exist a constant relationship between the overall mass transfer coefficient to the particle shape (e.g., described by the radius) and local concentration profile within the adsorbent. Liaw et al. [13] showed that a parabolic concentration of the form, $w(t,r) = a_0(t) + a_2(t)r^2$ as prescribed within the spherical particle, led to the well-known LDF model. Recently, Li and Yang [14] also demonstrated the use of the general profiles of the LDF model but modified with an exponent index n on $w(t,r)$, where n is an integer $\geqslant 2$ and commented that the parabolic profile of Liaw et al. [13] is one of the many possible local solutions. A recent article of Sircar and Hufton [15] highlighted that as long as the local concentration profile of the adsorbent is continuous, a constant relationship exist between $K_s a_v$ and the diffusional time, D_s/R^2, which is given by Eq. (1). This relation is originally derived by Glucckauf [16] where F_0 is 15 for spherical shapes of adsorbents:

$$F_0 = \frac{K_s a_v}{\left(\frac{D_s}{R^2}\right)} \tag{1}$$

In this paper, the adsorption rates of ethanol uptake onto the adsorbent ACF (A-20) for an assorted range of temperature have been measured which corresponds to useful temperatures expected of the operation of adsorption chillers, namely between 27 and 60 °C, respectively. Using a thermal-gravimetric analyzer (TGA) unit, instantaneous uptake measurements, as well as the adsorbent temperatures, are accurately recorded at regular time interval of 0.5 s. The chamber pressure of adsorbent is maintained constant during the experiments by a vacuum pump and a pressure-feedback modulating valve. Guided by the experimental measurements, a new concentration profile through the adsorbent is proposed in this paper where the exponent of the function for $w(t,r)$ has been found to be greater than what has been reported conventionally. The additional vapour-uptake, arising from the effect of the meso-pores within the uniformly distributed micro-pore structures of adsorbent material, can now be described by a variable k in the local concentration profile and this effect has been reported by Dubinin et al. [17]. However, they considered a statistical-moment method for the concentration profile that entails an infinite series solution for the kinetic curve.

2. Experiments

Fig. 1 shows a pictorial view of the experimental apparatus which comprises the TGA (CAHN TG 2121) unit, a water-heated evaporator, and a vacuum pump with the modulating valve. To measure the adsorption temperature, a thermocouple of type K is inserted into the reacting chamber near the bottom of the adsorbent or sample pan where both the adsorbent and the temperature sensor would be exposed to the same heater. The system pressure is controlled by the MKS pressure controller (type 651C) and a MKS-Baratron pressure sensor (type 631A) records the chamber pressure. The controller then operates the modulating vacuum valve. A diaphragm type vacuum pump is used to evacuate the system continuously, operating in concert with the pressure sensor and controller so as to maintain a pre-set chamber pressure condition. Fine porous meshes are mounted at the inlet and exit of the adsorbent chamber which provide damping for any pressure fluctuations arising from the modulating actions. During testing, the microbalance unit of the TGA is protected from any reactive gas by introducing a small amount of helium gas, which is injected from the top of the dome-shaped cover. As the sorbate is a condensable vapour, condensation is prevented by raising the tube and chamber wall temperatures, using an externally wrapped electric tape-heater.

A series of experimental runs have been carried out at different adsorption temperatures within a range from 27 to 60 °C. The evaporator, containing the liquid ethanol, is kept at a constant temperature of 15 °C by an adjustable temperature bath. Samples of ACF, typically about 71 mg in weight, are inserted into the reactor chamber of the TGA unit. Prior to each adsorption experiment, the sample is first regenerated under vacuum conditions but adsorbent is maintained at a temperature of 140 °C for several hours

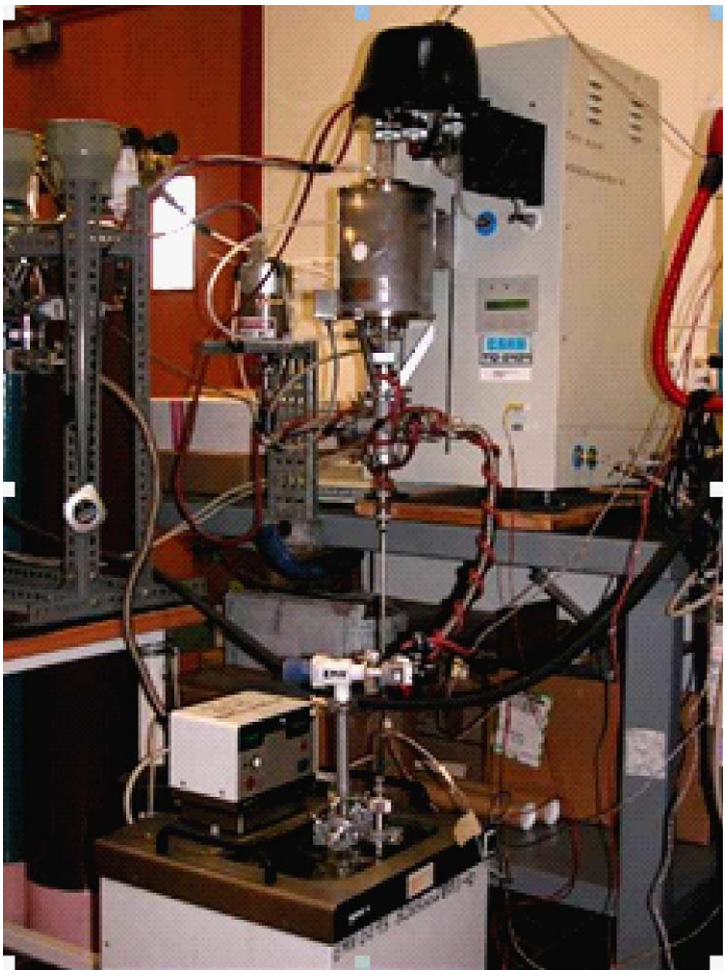

Fig. 1. Photograph of the experimental facility.

to ensure complete desorption. Gas extraction from the reacting chamber is conducted from the top section where it minimizes the mixing of ethanol and the helium gas. Separation of gases is also aided by the lower density of the helium gas.

Adsorption experiments commence when the evaporator (containing ethanol) valve is opened and ethanol vapour flows slowly to the reacting chamber through a porous plug. The system pressure is observed to increase from an initial pressure of 15 mbar (the lowest possible chamber pressure due to helium injection) to 30 mbar within a period of about 60 s and the chamber pressure remains constant throughout the adsorption experiment. The mass of adsorbed ethanol and the adsorbent temperatures are sampled and recorded at 0.5 s interval until the equilibrium conditions is attained.

3. Mathematical model

3.1. Semi-infinite model

It has been reported that during the initial phase of adsorption, surface diffusion coefficient follows the uptake behaviour of a semi-infinite medium of any particle shape and it is expressed by [12]:

$$\frac{w}{W} \approx \frac{2A}{V}\left(\frac{D_s t}{\pi}\right)^{1/2} \tag{2}$$

where A and V are the surface area and volume of the particles. Owing to the small pore diameters as compared to the ACF diameter, typically two to three orders smaller, the semi-infinite assumption is deemed justified. The diameter of the ACF is measured to be around 13 μm, as shown in the scanning electron micrograph (SEM) of Fig. 2. Considering a fiber to have a length, L, and a radius R, Eq. (2) can be customized as

$$\frac{w}{W} \approx \frac{4}{R}\left(\frac{D_s t}{\pi}\right)^{1/2} \tag{3}$$

where D_s/R^2 is the surface diffusion time constant. Thus, by evaluating the ethanol uptake with time from the TGA, Eq. (3) provides the methodology to evaluate the surface diffusion coefficient accurately. This approach has been adopted by many researchers [18–20] and reported to yield good results for the diffusion time constant.

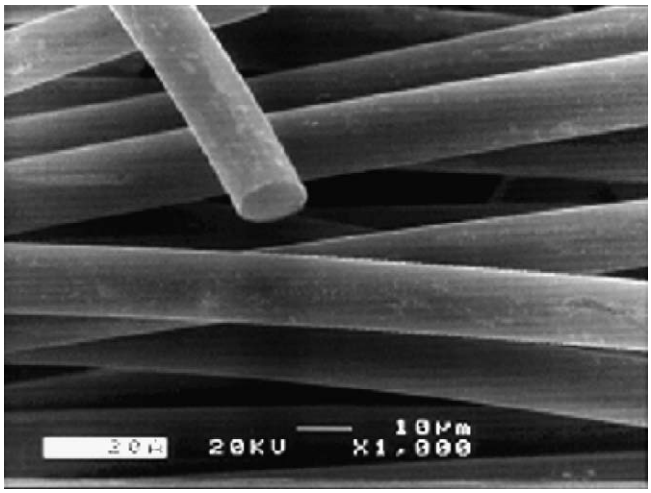

Fig. 2. Scanning electron micrographs (SEM) photographs of ACF (A-20).

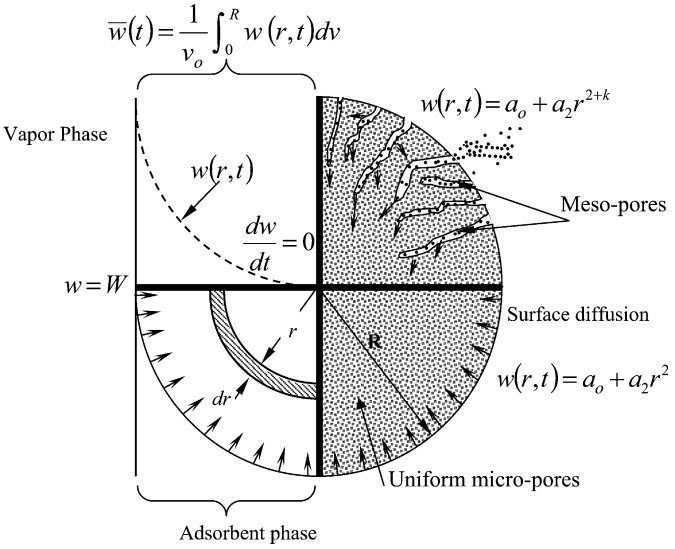

Fig. 3. Local concentration profiles for uniformly distributed micro-pores and meso-pores structures in ACF.

3.2. Linear driving force model

The local time dependent concentration of a sorbate within a cylindrical ACF having a uniform micro-pores structure could be described by the transient diffusion equation of the form given below [21]:

$$\frac{\partial w}{\partial t}=\frac{1}{r}\frac{\partial}{\partial r}\left(rD_s\frac{\partial w}{\partial r}\right) \tag{4}$$

where D_s is the surface diffusion coefficient and r is the radius of the ACF. Defining the volume-average sorbate concentration as $\bar{w}=\frac{1}{v_0}\int_0^R w\,\mathrm{d}v$, and on substitution of the parameters of a fiber volume, the elemental volume and differentiating it with respect to time, the volume average uptake of sorbate at any given time can be expressed as

$$\frac{\partial \bar{w}}{\partial t}=\frac{2}{R^2}\int_0^R \frac{\partial w}{\partial t}r\,\mathrm{d}r \tag{5}$$

The simple mathematical arrangement of Eqs. (4) and (5) provides the time-varying relation between volume-average sorbate uptake to the local concentration profile of the ACF, i.e.,

$$\frac{\partial \bar{w}}{\partial t}=\frac{2}{R^2}\int_0^R \left(\frac{1}{r}\frac{\partial}{\partial r}\left(rD_s\frac{\partial w}{\partial r}\right)\right)r\,\mathrm{d}r$$

or, simply when integrated gives

$$\frac{\partial \bar{w}}{\partial t}=\frac{2D_s}{R}\left[\frac{\partial w}{\partial r}\right]_{r=R} \tag{6}$$

The crucial step here is to assume a local distribution of sorbate through the cylinder. Classically, a quadratic function for the local distribution is used, i.e., $w=a_0+a_2r^2$, where the micro-pores are assumed to be uniformly distributed within the adsorbent, as shown in the lower quadrant of Fig. 3. However, as noted in the SEM Fig. 4, it is believed that there exist both meso- and micro-pores structures within the ACFs. To accommodate for the higher

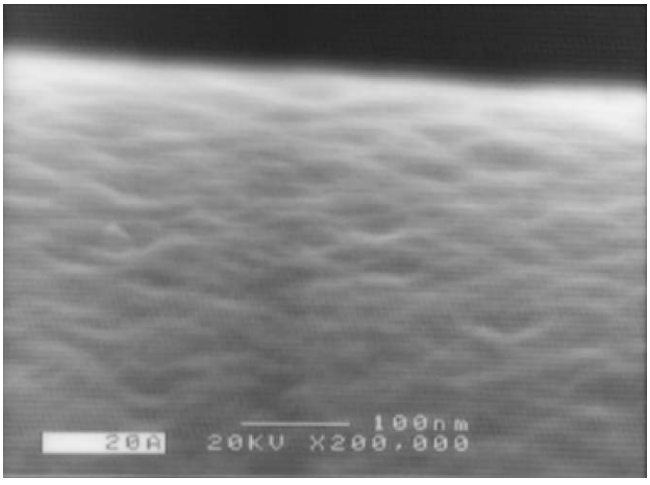

Fig. 4. SEM photographs of ACF (A-20) at higher magnification showing the dimples of meso-pores on the surface of ACF.

sorbate uptake, it is proposed that the local distribution function is assumed to have a form given as follows:

$$w=a_0+a_2r^{2+k} \tag{7}$$

where the parameter k accounts for the presence of meso- and micro-pores within the adsorbent, a_0 and a_2 are both function of time, r^{2+k} is any continues function within the fiber domain, satisfying the boundary conditions: $w=W$ at $r=R$, and $\frac{\partial w}{\partial r}=0$ at $r=0$. Substituting the local concentration profile, i.e., Eq. (7) the average uptake can be written by

$$\bar{w}=\frac{2}{R^2}\int_0^R \left(a_0+a_2r^{2+k}\right)r\,\mathrm{d}r \quad \text{or}$$
$$\bar{w}=a_0+\frac{2a_2}{4+k}R^{2+k} \tag{8}$$

Table 1
Coefficients of LDF approximation equation

Adsorbent particle shape	LDF equation constant without k	LDF equation constant with k
One-dimensional slab	3	$3+k$
Cylinder	8	$8+2k$
Sphere	15	$15+3k$

At equilibrium, the local concentration profile approaches the value at outer radius (R), $W = a_0 + a_2R^{2+k}$. Thus, the subtraction of $W - \bar{w}$ gives $a_2R^{2+k}(\frac{2+k}{4+k})$. From the local concentration distribution equation, one can also derive the concentration gradient at the ACF surface, i.e., $(\frac{\partial w}{\partial r})_{r=R} = (2+k)a_2R^{1+k}$, which can now be inserted into $W - \bar{w}$ to give the following:

$$W - \bar{w} = \frac{R}{(4+k)}\left(\frac{\partial w}{\partial r}\right)_{r=R} \tag{9}$$

Using Eqs. (6) and (9), they can be re-arranged to give

$$\frac{\partial \bar{w}}{\partial t} = \frac{(8+2k)D_s}{R^2}(W - \bar{w}) \tag{10}$$

which is similar in form to the conventional solution except that the parameter k is preserved and hence, the volume-average sorbate uptake could be enhanced due to the presence of meso- and micro-pores. It is highlighted that the same procedure could be applied to other adsorbent configurations such as the slab and sphere, and the results of the mathematical integration are listed in Table 1. Note that the solution for spherical adsorbent has the factor $(15+3k)$, that is quite similar to the conventional value of 15 only which is commonly used. However, this conventional value is obtained from quadratic concentration profile.

4. Results and discussion

Fig. 5 shows the instantaneous ethanol uptake onto the ACF (A-20) for 7 sets of isotherms by the TGA and the data are recorded at 0.5 s interval. At low temperature of 27 °C, the equilibrium uptake is achieved at 67% by mass within 2800 s. Similar asymptotic behaviour is also observed for isotherms 28 and 31.5 °C. As expected, the equilibrium ethanol uptake decreases with increasing temperatures. The TGA data, recorded at short time interval, makes it possible to estimate the experimental adsorption rate accurately throughout the transient. As it can be seen from the measured data, the slope of each isotherm increases with decreasing temperature. Thus, the

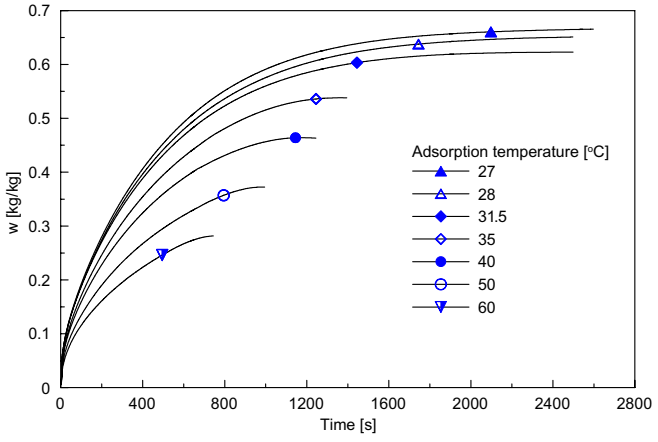

Fig. 5. Ethanol uptake on ACF (A-20) with time at assorted adsorption temperatures.

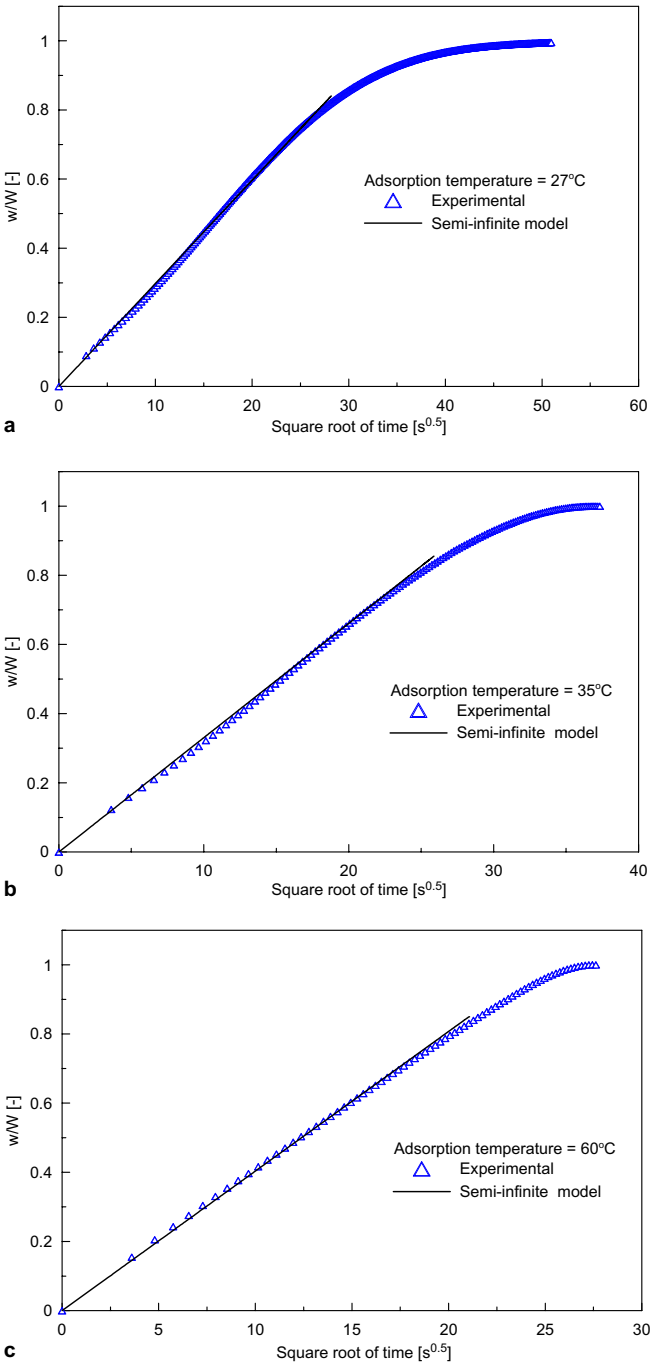

Fig. 6. Plots of fractional uptake versus $\sqrt{t}$ using the semi-infinite model.

adsorption rate ($\frac{\partial \bar{w}}{\partial t}$) is expected to increase with the decreasing adsorption temperature.

Using the semi-infinite model and the experimental data, the diffusion time constant, D_s/R^2 for each isotherm is calculated. To verify the semi-infinite model for the determination of diffusion time constant, selected isotherms of 27, 35 and 60 °C are compared by plotting the fractional uptake (w/W) versus the square root of time (t), as shown in Fig. 6. Each of these plots yields straight lines through the origin and the goodness of fit is valid up to about 80% of the total fractional uptake where the slope of the line yields the parameter $\frac{4}{\sqrt{\pi}}(\frac{D_s}{R^2})^{0.5}$. Thus, this procedure provides a simple method for the determination of diffusion time constant, D_s/R^2 of an isotherm.

The relationship between the overall mass transfer coefficient, $K_s a_v$, and D_s/R^2 is given by the LDF equation via the constant F_0, i.e., $K_s a_v = \frac{F_0 D_s}{R^2}$. Adsorption rate is calculated with a finite difference technique using the data from the experiments and the equilibrium uptake, W, is measured separately at equilibrium conditions. By plotting the dw/dt versus $(W - w)$ at each adsorption temperature, the overall mass transfer coefficient, $K_s a_v$, is then estimated. Using the diffusion time constant, D_s/R^2 (estimated by semi-infinite model), the numerical value of F_0 is evaluated. For the measured data of seven isotherms, the numerical value of F_0 is determined to be about 11 which implies that the value of k is 1.5 and it is valid for a temperature range from 27 to 60 °C and adsorption time of 600 s, corresponding to ethanol uptake up to 80% of the dry mass of adsorbent. It is noted that should the conventional parabolic concentration profile is used, then it would give a $F_0 = 8$, implying a lower ethanol uptake for the range of time and temperatures as the profile assumes only uniform micro-pores. This highlights the importance of the constant k in capturing the real concentration profile where the effects of both meso- and micro-pores are accounted for.

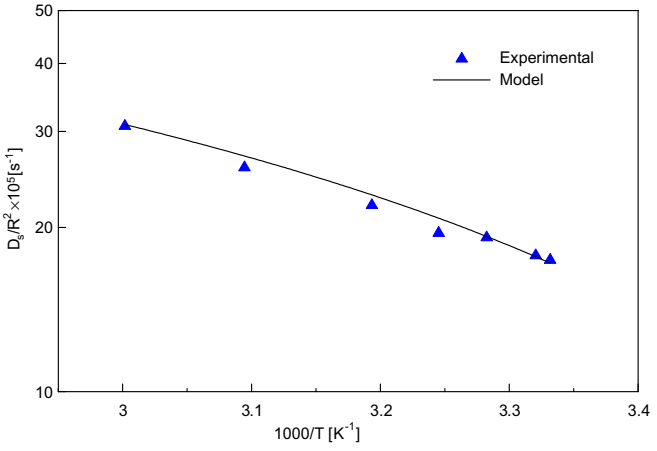

Fig. 7. A comparison of the diffusion time constant for a range of adsorption temperatures. The experimental uncertainty from TGA is small and no error bar is shown.

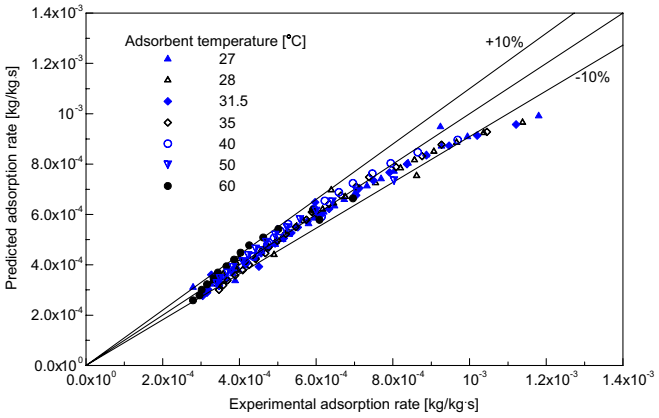

Fig. 8. A comparison of measured and predicted adsorption rates for all isotherms.

Fig. 7 shows the variation of the diffusion time constant with the adsorption temperatures. A good agreement is found between the experimentally measured results and theoretical predictions and they agree with the trend given by the classical Arrhenius equation. A comparison between measured and predicted adsorption rates are shown in Fig. 8, where the measured adsorption rates are determined by applying a finite difference calculation on the TGA data whilst the predictions are obtained by the LDF equation. A relatively good agreement for the adsorption rates is observed and the maximum percentage error for the bulk of data (from 7 isotherms) is found to be ±10%.

5. Conclusions

The adsorption rate of ethanol onto ACF (A-20) has been successfully measured using the TGA over a wide range of adsorption temperatures, typically from 27 to 60 °C, which is useful for the processes of adsorption chillers. It has been found that the semi-infinite model could capture the diffusion time constant, D_s/R^2 accurately for ethanol uptake up to 80% of the ACF's dry mass.

The authors have proposed a novel local concentration profile, $w(t,r) = a_0(t) + a_2(t)r^{2+k}$, which is effective in attributing the higher ethanol uptake due to the presence of meso- and micro-pores within the ACFs. The value of k in the local concentration profile has been independently validated using the measured data and is found to be about 1.5 when F_0 is 11 which is much higher than the conventional value of 8. The value of k is also valid for the wide range of adsorption temperatures.

By combining the values of k and D_s/R^2, the linear driving force (LDF) model is now proposed to be of the form, i.e., $\frac{\partial \bar{w}}{\partial t} = \frac{(8+2k)D_s}{R^2}(W - \bar{w})$ which is valid for a cylindrical adsorbent. The numerical values of k and D_s/R^2 are valid over a wide range of adsorption temperatures as well as the adsorbent surfaces with meso- and micro-pores. The authors would like to infer similar LDF models for one-dimensional slab and spherical shapes where the parenthesis terms are $(3 + k)$ and $(15 + 3k)$, respectively.

Acknowledgement

The authors acknowledge the financial support under the ASTAR SERC grant of Singapore (Project No. 0221010035).

References

[1] M. El-Merraoui, M. Aoshima, K. Kaneko, Micropore size distribution of activated carbon fiber using the density functional theory and other methods, Langmuir 16 (9) (2000) 4300–4303.
[2] M. Suzuki, Activated carbon fiber: Fundamentals and applications, Carbon 32 (4) (1994) 577–586.
[3] S. Sircar, T.C. Golden, M.B. Rao, Activated carbon for gas separation and storage, Carbon 34 (1) (1996) l–12.
[4] K.R. Matranga, A.L. Myers, E.D. Glandt, Storage of natural gas by adsorption on activated carbon, Chem. Eng. Sci. 47 (7) (1992) 1569–1579.
[5] D. Mehandjiev, E. Bekyarova, M. Khristova, Study of Ni-impregnated active carbon, J. Colloid Interface Sci. 192 (2) (1997) 440–446.
[6] R.Z. Wang, J.P. Jia, Y.H. Zhu, Y. Teng, J.Y. Wu, J. Cheng, Q.B. Wang, Study on a new solid absorption refrigeration pair: active carbon fiber–methanol pair, J. Sol. Energy Eng., Trans. ASME 119 (1997) 214–218.
[7] L.L. Vasiliev, D.A. Mishkinis, A.A. Antukh, L.L. Vasiliev Jr., Solar–gas solid sorption heat pump, Appl. Therm. Eng. 21 (5) (2001) 573–583.
[8] M. Kanamori, M. Hiramatsu, K. Katsurayama, F. Watanabe, M. Hasatani, Production of cold heat energy by alcohol/activated carbon adsorption heat pump with disk module-type adsorber, J. Chem. Eng. Jpn. 30 (3) (1997) 434–439.
[9] I.I. El-Sharkawy, K. Kuwahara, B.B. Saha, S. Koyama, K.C. Ng, Experimental investigation of activated carbon fibers/ethanol pairs for adsorption cooling system application, Appl. Therm. Eng. 26 (8–9) (2006) 859–865.
[10] B.B. Saha, S. Koyama, K.C.A. Alam, Y. Hamamoto, A. Akisawa, T. Kashiwagi, K.C. Ng, H.T. Chua, Isothermal adsorption measurement for the development of high performance solid sorption cooling system, Trans. JSRAE 20 (3) (2003) 421–427.
[11] M.A. Buzanowski, R.T. Yang, Extended linear driving-force approximation for intraparticle diffusion rate including short times, Chem. Eng. Sci. 44 (11) (1989) 2683–2689.
[12] D.M. Ruthven, Principles of Adsorption and Adsorption Processes, John Willy & Sons, Inc., 1984, pp. 128–130.
[13] C.H. Liaw, J.S.P. Wang, R.H. Greenkorn, K.C. Chao, Kinetics of fixed-bed adsorption: a new solution, AIChE J. 25 (1979) 376.
[14] Z. Li, R.T. Yang, Concentration profile for linear driving force model for diffusion in a particle, AIChE J. 45 (1) (1999) 196–200.
[15] S. Sircar, J.R. Hufton, Intraparticle adsorbate concentration profile for linear driving force model, AIChE J. 46 (3) (2000) 659–660.
[16] E. Glueckauf, Formula for diffusion into sphere and their application to chromatography, Trans. Faraday Soc. 51 (1955) 1540–1551.
[17] M.M. Dubinin, I.T. Erashko, O. Kadlec, V.I. Ulin, A.M. Voloshchuk, P.P. Zolotarev, Kinetics of physical adsorption by carbonaceous adsorbents of biporous structure, Carbon 13 (3) (1975) 193–200.
[18] D.R. Garg, D.M. Ruthven, The effect of the concentration dependence of diffusivity on zeolitic sorption curves, Chem. Eng. Sci. 27 (2) (1972) 417–423.
[19] H. Yucel, D.M. Ruthven, Diffusion in 4A zeolite; study of the effect of crystal size, J. Chem. Soc. Faraday Trans. I 76 (1980) 60–70.
[20] H. Yucel, D.M. Ruthven, Diffusion in 5A zeolite; study of the effect of crystal size, J. Chem. Soc. Faraday Trans. I 76 (1980) 71–83.
[21] I.J. Crank, The Mathematics of Diffusion, second ed., Oxford University press, 1975, pp. 67–88.